HAL
open science

Nonadiabatic Kohn Anomaly in Heavily Boron-Doped Diamond

Fabio Caruso, Moritz Hoesch, Philipp Achatz, Jorge Serrano, Michael Krisch, Etienne Bustarret, Feliciano Giustino

To cite this version:

Fabio Caruso, Moritz Hoesch, Philipp Achatz, Jorge Serrano, Michael Krisch, et al.. Nonadiabatic Kohn Anomaly in Heavily Boron-Doped Diamond. Physical Review Letters, 2017, 119 (1), pp.017001. 10.1103/PhysRevLett.119.017001 . hal-01620961

HAL Id: hal-01620961

https://hal.science/hal-01620961

Submitted on 22 Oct 2017

HAL is a multi-disciplinary open access archive for the deposit and dissemination of scientific research documents, whether they are published or not. The documents may come from teaching and research institutions in France or abroad, or from public or private research centers.

L'archive ouverte pluridisciplinaire **HAL**, est destinée au dépôt et à la diffusion de documents scientifiques de niveau recherche, publiés ou non, émanant des établissements d'enseignement et de recherche français ou étrangers, des laboratoires publics ou privés.

Non-adiabatic Kohn Anomaly in Heavily Boron-doped Diamond

Fabio Caruso,[1] Moritz Hoesch,[2] Philipp Achatz,[3] Jorge Serrano,[4]
Michael Krisch,[5] Etienne Bustarret,[3] and Feliciano Giustino[1,*]

[1] *Department of Materials, University of Oxford, Parks Road, Oxford, OX1 3PH, United Kingdom*
[2] *Diamond Light Source, Harwell Campus, Didcot OX11 0DE, United Kingdom*
[3] *Univ. Grenoble Alpes, CNRS, Inst. NEEL, F-38000 Grenoble, France*
[4] *Yachay Tech University, School of Physical Sciences and Nanotechnology, 100119-Urcuquí, Ecuador*
[5] *European Synchrotron Radiation Facility, 6 rue Jules Horowitz, 38043 Grenoble Cedex, France*

(Dated: April 27, 2017)

We report evidence of a non-adiabatic Kohn anomaly in boron-doped diamond, using a joint theoretical and experimental analysis of the phonon dispersion relations. We demonstrate that standard calculations of phonons using density functional perturbation theory are unable to reproduce the dispersion relations of the high-energy phonons measured by high-resolution inelastic x-ray scattering. On the contrary, by taking into account non-adiabatic effects within a many-body field-theoretic framework, we obtain excellent agreement with our experimental data. This result indicates a breakdown of the Born-Oppenheimer approximation in the phonon dispersion relations of boron-doped diamond.

The Kohn anomaly (KA) is one of the most striking manifestations of the influence of electron-phonon coupling on the lattice dynamics of metals [1]. KAs result from the screening of lattice vibrations by virtual electronic excitations across the Fermi surface [2], and manifest themselves through distinctive dips in the phonon dispersion relations. The existence of KAs was confirmed by inelastic neutron scattering experiments [3] shortly after Kohn's theoretical prediction [1]. Since then KAs have been observed in a number of metals [4–6], conventional superconductors [7, 8], as well as superconducting semiconductors [9].

Interest in KAs was recently re-ignited by the discovery of *non-adiabatic* KAs in carbon materials, such as graphene [10, 11], carbon nanotubes [12, 13], and graphite intercalation compounds [14–16]. At variance with adiabatic KAs, which are well described in the adiabatic Born-Oppenheimer approximation [1], non-adiabatic KAs arise when the electronic screening takes place on timescales which are comparable to the period of lattice vibrations, and signal the breakdown of the Born-Oppenheimer approximation. In the majority of current first-principles calculations, these non-adiabatic effects are ignored on the grounds that they should be of the order of m/M, with m the electron mass and M the characteristic nuclear mass. While the calculations of non-adiabatic phonon linewidths may be performed using standard implementations [17], first-principles studies of renormalization effects on the phonon dispersions due to non-adiabaticity are extremely challenging, and have thus far been confined to low-dimensional compounds. In particular, for metallic compounds characterized by a two-dimensional, quasi-two-dimensional, or one-dimensional structure it has been shown that non-adiabatic effects can alter significantly the phonon dispersion relations [10–16, 18]. Instead, for three-dimensional bulk metals, it has been suggested that non-adiabatic effects might be too small to be observable in experiment [15].

The strong coupling between electrons and longitudinal optical (LO) phonons in diamond, manifested for instance by a 0.6 eV zero-point motion band-gap renormalization [19–21] and the emergence of type-II superconductivity for sufficiently high B-doping [22], make it a good candidate for the observation of non-adiabatic effects in the phonon dispersions. Pristine diamond has previously attracted considerable interest due to the anomalous overbending of the optical phonon branch [23]. In presence of B-dopants, the electron-phonon interaction induces a softening of the LO phonons at long wavelengths, and a concomitant broadening of the spectral lines [9, 24]. These effects are taken to be the signatures of a doping-induced KA. The measured softening is found to be between 4 and 7 meV for B-doping concentrations of 10^{20}-10^{21} cm^{-3} [9, 24]. Intriguingly, first-principles calculations [25–29] gave considerably more pronounced phonon softening, in the range of 20 to 30 meV. This unusually large discrepancy between experiment and theory remains an outstanding question in the physics of superconducting diamond [30]. This led us to formulate the hypothesis that in order to explain the measured KA in diamond it might be necessary to invoke non-adiabatic effects.

In this work we analyze the dispersion relations of the longitudinal-optical (LO) phonons of B-doped diamond using state-of-the-art first-principles calculations and inelastic x-ray scattering (IXS) measurements. By comparing theory and experiment we demonstrate that the non-adiabatic correction to the LO phonon energy is indeed very large, up to 10 meV. After including non-adiabatic effects within a field-theoretic framework, we obtain an unprecedented agreement between theory and experiment, and we resolve the discrepancy between earlier theoretical works and measured phonon dispersions.

Our results demonstrate a breakdown of the adiabatic Born-Oppenheimer approximation in the phonon dispersion relations of boron-doped diamond, revealing that these effects may be sizeable also in three-dimensional bulk compounds.

The B-doped diamond samples were prepared by microwave plasma-enhanced chemical vapor deposition (MPCVD) from a hydrogen-rich gas phase with added diboran (B_2H_6). The samples were grown homoepitaxially on type Ib synthetic crystals with (001) oriented surfaces at thicknesses of 25 ± 5 μm [31]. The boron concentration was determined from secondary ion mass spectroscopy (SIMS) of $^{11}B^-$, $^{12}C^-$ and $^{11}B^{12}C^-$ ions. For a B-doping concentration of $1.4 \cdot 10^{21}$ cm^{-3}, the samples exhibit superconducting behaviour with critical temperature $T_c = 2.8$ K. IXS spectra were measured at beamline ID28 at the European Synchrotron Radiation Facility (ESRF) with an energy resolution of 3.2 meV. The samples were aligned with the beam directed parallel to the surface and passing through the substrate or the B-doped diamond film, for measurements of pristine diamond and B-doped diamond, respectively. The scattering vector $\mathbf{Q}$ was varied from $(2.06, 0, 0)2\pi/a$ (close to Γ) to $(3, -0.12, 0)2\pi/a$ (close to X), with $a = 3.67$ Å. The small deviations in the $(0, k, 0)$ direction are given in Supplemental Table 1 [32]. The measured IXS spectra are shown in Fig. 1 (c)-(e) as heat maps, and in Supplemental Fig. 1 as individual scans [32]. For the undoped case, our measurements are in excellent agreement with previous experimental data [33].

Non-adiabatic phonon dispersions were computed from first-principles within the many-body theory of electron-phonon coupling. Non-adiabatic effects were accounted for via the phonon self-energy $\Pi^{\rm NA}_{\mathbf{q}\nu}$ [17]:

$$\hbar\Pi^{\rm NA}_{\mathbf{q}\nu}(\omega) = 2\sum_{mn}\int \frac{d\mathbf{k}}{\Omega_{\rm BZ}} g^{\rm b}_{mn,\nu}(\mathbf{k},\mathbf{q}) g^{*}_{mn,\nu}(\mathbf{k},\mathbf{q}) \times \left[\frac{f_{n\mathbf{k}} - f_{m\mathbf{k}+\mathbf{q}}}{\epsilon_{m\mathbf{k}+\mathbf{q}} - \epsilon_{n\mathbf{k}} - \hbar(\omega + i\eta)} - \frac{f_{n\mathbf{k}} - f_{m\mathbf{k}+\mathbf{q}}}{\epsilon_{m\mathbf{k}+\mathbf{q}} - \epsilon_{n\mathbf{k}}}\right], \quad (1)$$

where $\epsilon_{n\mathbf{k}}$ and $f_{n\mathbf{k}}$ denote single-particle energies and Fermi-Dirac occupation factors, η is a positive infinitesimal, and $\Omega_{\rm BZ}$ is the Brillouin zone volume. The *screened* electron-phonon matrix elements $g_{mn,\nu}(\mathbf{k},\mathbf{q})$ were obtained as $g_{mn,\nu}(\mathbf{k},\mathbf{q}) = (\hbar/2M\omega_{\mathbf{q}\nu})^{1/2}\langle\psi_{m\mathbf{k}+\mathbf{q}}|\partial_{\mathbf{q}\nu}V|\psi_{n\mathbf{k}}\rangle$, where $\psi_{n\mathbf{k}}$ denote Kohn-Sham single-particle eigenstates, M the C mass, and $\partial_{\mathbf{q}\nu}V$ the derivative of the self-consistent potential associated with the ν-th phonon mode with wavevector $\mathbf{q}$ and energy $\hbar\omega_{\mathbf{q}\nu}$. $g_{mn,\nu}(\mathbf{k},\mathbf{q})$ is obtained from the *bare* matrix element $g^{\rm b}_{mn,\nu}(\mathbf{k},\mathbf{q})$ by screening the variation of the ionic potential using the electronic dielectric function. Here we calculate $g^{\rm b}_{mn,\nu}(\mathbf{k},\mathbf{q})$ by unscreening $g_{mn,\nu}(\mathbf{k},\mathbf{q})$ and neglect local-field effects for simplicity. Equation (1) accounts for both the *screened* and the *bare* electron-phonon vertices (g and $g^{\rm b}$) and it thus avoids the approximation employed in previous first-principles calculations, whereby the matrix elements $g^{\rm b}_{mn,\nu}(\mathbf{k},\mathbf{q})g^{*}_{mn,\nu}(\mathbf{k},\mathbf{q})$ were replaced by $|g_{mn,\nu}(\mathbf{k},\mathbf{q})|^2$ [17]. The non-adiabatic phonon dispersions, that is, the dispersions modified by the phonon self-energy of Eq. (1), were extracted directly from the phonon spectral function [34]:

$$A_{\mathbf{q}\nu}(\omega) = \pi^{-1}{\rm Im}\left[\frac{2\omega_{\mathbf{q}\nu}}{\omega^2 - \omega^2_{\mathbf{q}\nu} - 2\omega_{\mathbf{q}\nu}\Pi^{\rm NA}_{\mathbf{q}\nu}(\omega)}\right]. \quad (2)$$

Equation (2), which constitutes the phonon counterpart of the electronic spectral function [2], exhibits peaks at the non-adiabatic phonon frequencies $\Omega_{\mathbf{q}\nu}$ given by:

$$\Omega^2_{\mathbf{q}\nu} \simeq \omega^2_{\mathbf{q}\nu} + 2\omega_{\mathbf{q}\nu}{\rm Re}\,\Pi^{\rm NA}_{\mathbf{q}\nu}(\Omega_{\mathbf{q}\nu}), \quad (3)$$

with a full-width at half-maximum $\Gamma_{\mathbf{q}\nu} = 2\hbar\,{\rm Im}\Pi^{\rm NA}_{\mathbf{q}\nu}(\Omega_{\mathbf{q}\nu})$. Non-adiabatic phonon spectral functions obtained from Eq. (2) are reported in Fig. 1 (f)-(h), whereas the phonon dispersions derived from Eq. (3) are shown in Fig. 1 (i)-(k).

Inspection of Eq. (1) reveals that non-adiabatic effects may become important whenever the transition energies between occupied and empty electronic states $(\epsilon_{m\mathbf{k}+\mathbf{q}} - \epsilon_{n\mathbf{k}})$ approach the characteristic phonon energy $\hbar\omega_{\mathbf{q}\nu}$. As in solids $\hbar\omega_{\mathbf{q}\nu}$ is typically $\lesssim 100$ meV, this condition is only satisfied in metals, doped semiconductors, and narrow-gap semiconductors, whereby low-energy intra-band transitions may be excited. Therefore, in these systems one may expect to observe (i) phonon damping effects, with a characteristic timescale set by the phonon lifetime $\tau_{\mathbf{q}\nu} = \hbar/\Gamma_{\mathbf{q}\nu}$; and (ii) a renormalization of the adiabatic phonon frequencies, arising from the finite value of ${\rm Re}\Pi^{\rm NA}_{\mathbf{q}\nu}(\Omega_{\mathbf{q}\nu})$ in Eq. (3). On the other hand, the standard Born-Oppenheimer approximation is recovered in the limit $\Pi^{\rm NA}_{\mathbf{q}\nu} = 0$.

The phonon dispersions of pristine diamond in the adiabatic approximation are presented in Fig. 1 (b) for momenta along the L-Γ-X path. The acoustic and optical phonon branches, which correspond to the in- and out-of-phase oscillation of the diamond sublattices, are denoted as AP and OP in Fig. 1 (b). Pristine diamond is an insulator with a fundamental band gap $E_g = 5.4$ eV [35, 36] and the large optical phonon energy of $\hbar\omega_{\rm ph} = 164$ meV reflects the stiffness of its covalent bonds. Since $E_g \gg \hbar\omega_{\rm ph}$, non-adiabatic effects are relatively unimportant, and the non-adiabatic corrections are smaller than 0.4 meV, see Fig. 1 (i). The resulting phonon dispersions are in excellent agreement with our measured IXS spectrum in Fig. 1 (c), in line with the notion that phonons in wide band-gap insulators are well described in the adiabatic approximation.

To quantify the importance of non-adiabaticity for undoped semiconductors and insulators, we derive a simple estimate of the energy renormalization. In the limit of non-dispersive electronic bands, one may replace

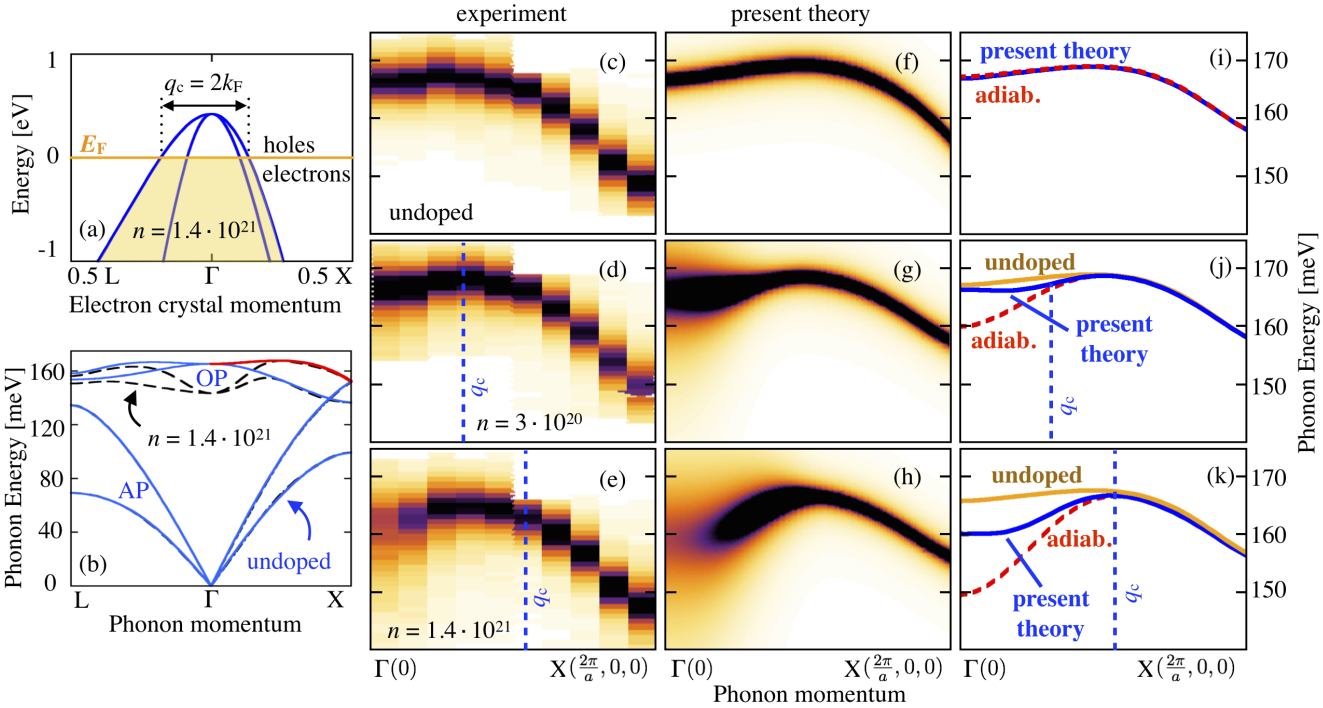

Figure 1. (a) Density-functional theory band structure of diamond for a B concentration of $1.4 \cdot 10^{21}$ cm^{-3}. (b) Adiabatic phonon dispersions of pristine (blue lines) and B-doped diamond (dashed black lines) for momenta along L-Γ-X, as obtained from density-functional perturbation theory. (c)-(e) Measured IXS spectra of pristine and B-doped diamond. The critical momentum for the onset of the KA, $q_c = 2k_F$, is indicated by vertical dashed lines, see also (a). (f)-(h) Non-adiabatic spectral function, obtained from Eqs. (1)-(2), for the LO phonon of (c) pristine and (d)-(e) B-doped diamond along Γ-X. The phonon branch considered here is marked by the red line in panel (b). (i)-(k) Phonon energies obtained from Eq. (3) in the adiabatic approximation ($\Pi^{\rm NA}_{\mathbf{q}\nu} = 0$), and from the fully non-adiabatic theory (present theory). Non-adiabatic phonon dispersions of undoped diamond are reported for comparison. All doping concentrations are in units of cm^{-3}.

$\epsilon_{m\mathbf{k}+\mathbf{q}} - \epsilon_{n\mathbf{k}} = E_g$ in Eq. (1). If we further assume an Einstein model for the optical phonons $\hbar\omega_{\mathbf{q}\nu} = \hbar\omega_{\rm E}$ and we restrict ourselves to the limit $\hbar\omega_{\rm E} \ll E_g$, the term in squared bracket in Eq. (1) reduces to $\hbar\omega_{\rm E}/E_g^2$ to first order. An explicit approximation for Eq. (1) then is promptly obtained: $\hbar\Pi = 2\epsilon_\infty g^2 \hbar\omega_{\rm E}/E_g^2$, with ϵ_∞ being the dielectric constant and g the average electron-phonon matrix element. For diamond, using $\epsilon_\infty = 5.44$, $E_g = 5.4$ eV, $\hbar\omega_{\rm E} = 0.16$ eV, and $g = 0.1$ eV, we obtain $\hbar\Pi = 0.5$ meV, which is consistent with the first principles calculations shown in Fig. 1 (i).

As compared to the undoped case, the IXS spectra of B-doped diamond in Figs. 1 (d)-(e) exhibit a red-shift of the LO phonon energy and an increase of the phonon linewidth close to Γ, which indicate the emergence of a doping-induced KA. To quantify the effect of doping on the phonon energy, we define the phonon softening parameter $\Delta\Omega_{\mathbf{q}\nu}(n) = \Omega_{\mathbf{q}\nu}(0) - \Omega_{\mathbf{q}\nu}(n)$, where $\Omega_{\mathbf{q}\nu}(n)$ denotes the phonon frequency at a carrier density n. The softening and linewidth become more pronounced with the increase of doping concentration. The KA is observed only for wave-vectors smaller than a critical cut-off value $q_c = 2k_{\rm F}$, with $k_{\rm F}$ being the Fermi momentum, which corresponds to the maximum momentum transfer for electron-phonon scattering on the Fermi surface, see Fig. 1 (a) [1]. Using the Fermi momentum of the homogeneous electron gas model, $k_{\rm F} = (3\pi^2 n/N_m)^{\frac{1}{3}}$, where $N_m = 3$ is the degeneracy of the valence-band top of diamond, we obtain $q_c = 0.3$ and 0.5 Å^{-1} for doping levels of $3 \cdot 10^{20}$ and $1.4 \cdot 10^{21}$ cm^{-3}, respectively. These values are marked by vertical dashed lines in Fig. 1 (d)-(e) and (j)-(k).

For momenta $q < q_c$ we find adiabatic phonon dispersions consistent with previous works [25, 28, 29]. As reported in Refs. 9 and 29, however, the adiabatic approximation leads to a systematic underestimation of the phonon energy as compared to experiment, which becomes more pronounced with the increase of doping concentration. Conversely, fully non-adiabatic calculations yield phonon energies in excellent agreement with IXS, as revealed by the comparison between Fig. 1 (d)-(e) and (j)-(k). To quantify the importance of non-adiabatic effects, we compare in Fig. 2 the softening $\Delta\Omega_{\mathbf{q}\nu}$ and the lineshapes for the LO phonon of B-doped diamond, as obtained from IXS, from the adiabatic approximation, and from fully non-adiabatic calculations. Above

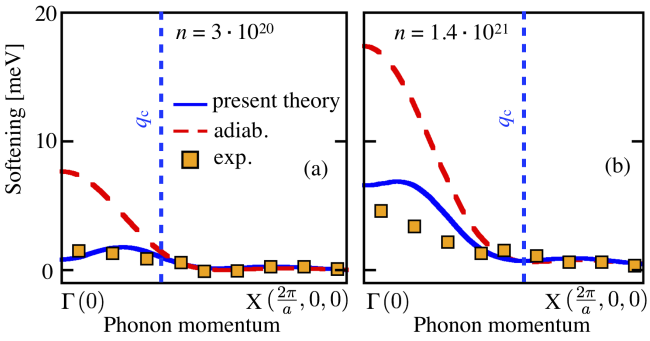

Figure 2. Energy renormalization of the longitudinal optical phonons of diamond, for doping concentrations of (a) $1.4 \cdot 10^{21}$ cm^{-3} and (b) $3 \cdot 10^{20}$ cm^{-3}: experiment (squares), adiabatic (dashed red line) and non-adiabatic theory (blue line).

the threshold $q > q_c$ for the onset of the KA, theory and experiment yield a phonon softening smaller than 1 meV for all doping concentrations. For $q < q_c$, instead, the positive phonon softening reflects the red-shift of the phonon frequency induced by electron-phonon interactions. Figure 2 (a)-(b) reveal that the adiabatic approximation overestimates the experimental softening by as much as 300% close to Γ. At a doping concentration of $1.4 \cdot 10^{21}$ cm^{-3}, for instance, the adiabatic LO phonon energy at Γ is softened by $\Delta\Omega_\Gamma^{\rm adiab} = 22$ meV, whereas from IXS we have $\Delta\Omega_\Gamma^{\rm exp} = 5.3$ meV. The non-adiabatic theory, on the other hand, yields a softening in excellent agreement with experiment: for instance, we obtain $\Delta\Omega_\Gamma^{\rm NA} = 7$ meV for the same doping level. These results are further corroborated by considering an Einstein phonon model coupled to a homogeneous electron gas with parabolic dispersion $\epsilon_{\mathbf{k}} = \hbar^2 k^2/2m^*_{\rm dos}$, with $m^*_{\rm dos} = 1.18$ being the density-of-state effective mass of diamond. Within these approximations Eq. (1) reduces to $\hbar\Pi = 2g^2\epsilon_\infty[\chi_0(\omega_{\rm E}) - \chi_0(0)]$, with $\chi_0(\omega)$ being the long-wavelength limit ($\mathbf{q} \to 0$) of the Lindhard function [2]. For diamond, using $\hbar\omega_{\rm E} = 0.16$ eV, $g = 0.1$ eV, $m^*_{\rm dos} = 1.18$, and $\epsilon_\infty = 5.44$, we obtain $\hbar\Pi \simeq 8$ meV for $n = 1.4 \cdot 10^{21}$ cm^{-3}, in agreement with our ab initio calculations.

These features are also nicely reproduced by the phonon dispersions reported in Fig. 1 (g)-(h), confirming the non-adiabatic character of the KA. Owing to the undamped nature of phonons in the adiabatic approximation (here we ignore phonon-phonon interactions), the adiabatic spectral functions are characterized by infinitesimal linewidths. The non-adiabatic spectra, on the other hand, correctly reproduce (i) the increase of spectral linewidth with doping concentration, and (ii) the decrease of the linewidth with phonon momentum as shown in Fig. 1 (c)-(h) and in Fig. S3 [32]. The resulting spectral lineshapes are in good qualitative agreement with IXS, suggesting that electron-phonon scattering constitutes the primary mechanism for LO phonon damping in superconducting diamond.

The pronounced non-adiabatic character of the lattice dynamics in doped diamond indicates a breakdown of the adiabatic Born-Oppenheimer approximation. This effect may be explained by considering the timescales involved: while LO phonons oscillate with a period $\tau_{\rm ph} = 25$ fs, the timescale of electronic screening τ_s is set by the plasma frequency $\omega_{\rm pl}$ via $\tau_s = 2\pi/\omega_{\rm pl} = 2\pi(4\pi n/m^*\epsilon_\infty)^{-1/2}$, with m^* being the carrier effective mass. Using this expression, we find $\tau_s = 9$ and 4 fs for $n = 3 \cdot 10^{20}$ and $1.4 \cdot 10^{21}$ cm^{-3}, respectively, which are compatible with the results of optical measurements [37, 38]. As screening operates on timescales that approach the characteristic phonon period, the assumptions underlying the Born-Oppenheimer approximation are not valid, and we see the emergence of strong non-adiabatic coupling.

As a first step to explore the consequences of non-adiabaticity in B-doped diamond, we examine the superconducting critical temperature $T_{\rm c}$ using McMillan's formula [39, 40]: $T_{\rm c} = \langle\omega\rangle/1.2\exp\{-1.04(1+\lambda)/[\lambda - \mu^*(1+0.62\lambda)]\}$, where λ is the electron-phonon coupling strength, and $\langle\omega\rangle$ the logarithmic average of the phonon frequency. Following Refs. [40, 41], the Coulomb pseudopotential μ^* is set to the standard value of 0.11. Noting that $\lambda \propto \omega_{\mathbf{q}\nu}^{-2}$ [17], a small change in the phonon frequency as introduced by the adiabatic approximation, may induce a large modification of $T_{\rm c}$. At a doping concentration of $1.4 \cdot 10^{21}$ cm^{-3}, for instance, the adiabatic approximation underestimates the LO phonon frequency in diamond by $\sim 10\%$. In turn, this results into an overestimation of λ by $\sim 20\%$. This inaccuracy is amplified by the exponential dependence of $T_{\rm c}$ on λ, leading to an overestimation of the critical temperature by up to 50%. Non-adiabatic effects thus carry important implications for the theoretical prediction of $T_{\rm c}$, and should be considered in future studies.

In conclusion, by combining first-principles calculations of the electron-phonon interaction and high-resolution IXS experiments, we demonstrated the emergence of a non-adiabatic KA in superconducting diamond. Beside resolving a long-standing discrepancy between theory and experiment, these findings reveal that a breakdown of the Born-Oppenheimer approximation may lead to sizeable renormalization effects in the phonon dispersions of three-dimensional crystals. Our work calls for a systematic investigation of non-adiabatic effects and Kohn anomalies in the phonon dispersions of three-dimensional heavily doped semiconductors as well as superconducting oxides.

We wish to thank L. Ortéga for help with the x-ray diffraction characterisation of the samples and F. Jomard for calibration of the B-concentration by secondary ion mass spectrometry (SIMS) and depth profiling a few μm. The research leading to these results has received fund-

ing from the Leverhulme Trust (Grant RL-2012-001), the European Union's Horizon 2020 research and innovation programme under grant agreement No. 696656 - GrapheneCore1, and the UK Engineering and Physical Sciences Research Council (Grant No. EP/J009857/1). Supercomputing time was provided by the University of Oxford Advanced Research Computing facility (http://dx.doi.org/10.5281/zenodo.22558) and the ARCHER UK National Supercomputing Service. We acknowledge the ESRF for granting use of beamline ID28, which contributed to the results presented here.

* feliciano.giustino@materials.ox.ac.uk

[1] W. Kohn, Phys. Rev. Lett. **2**, 393 (1959).
[2] G. Mahan, *Many-Particle Physics* (Springer, 2000).
[3] B. N. Brockhouse, K. R. Rao, and A. D. B. Woods, Phys. Rev. Lett. **7**, 93 (1961).
[4] B. N. Brockhouse, T. Arase, G. Caglioti, K. R. Rao, and A. D. B. Woods, Phys. Rev. **128**, 1099 (1962).
[5] Y. Nakagawa and A. D. B. Woods, Phys. Rev. Lett. **11**, 271 (1963).
[6] S. H. Koenig, Phys. Rev. **135**, A1693 (1964).
[7] A. Q. R. Baron, H. Uchiyama, Y. Tanaka, S. Tsutsui, D. Ishikawa, S. Lee, R. Heid, K.-P. Bohnen, S. Tajima, and T. Ishikawa, Phys. Rev. Lett. **92**, 197004 (2004).
[8] P. Aynajian, T. Keller, L. Boeri, S. M. Shapiro, K. Habicht, and B. Keimer, Science **319**, 1509 (2008).
[9] M. Hoesch, T. Fukuda, J. Mizuki, T. Takenouchi, H. Kawarada, J. P. Sutter, S. Tsutsui, A. Q. R. Baron, M. Nagao, and Y. Takano, Phys. Rev. B **75**, 140508 (2007).
[10] M. Lazzeri and F. Mauri, Phys. Rev. Lett. **97**, 266407 (2006).
[11] S. Pisana, M. Lazzeri, C. Casiraghi, A. K. Novoselov, K. S. Geim, A. C. Ferrari, and F. Mauri, Nat. Mater. **6**, 198 (2007).
[12] N. Caudal, A. M. Saitta, M. Lazzeri, and F. Mauri, Phys. Rev. B **75**, 115423 (2007).
[13] S. Piscanec, M. Lazzeri, J. Robertson, A. C. Ferrari, and F. Mauri, Phys. Rev. B **75**, 035427 (2007).
[14] M. Calandra, M. Lazzeri, and F. Mauri, Physica C **456**, 38 (2007).
[15] A. M. Saitta, M. Lazzeri, M. Calandra, and F. Mauri, Phys. Rev. Lett. **100**, 226401 (2008).
[16] M. Calandra, G. Profeta, and F. Mauri, Phys. Rev. B **82**, 165111 (2010).
[17] F. Giustino, Rev. Mod. Phys. **89**, 015003 (2017).
[18] M. Leroux, I. Errea, M. Le Tacon, S.-M. Souliou, G. Garbarino, L. Cario, A. Bosak, F. Mauri, M. Calandra, and P. Rodière, Phys. Rev. B **92**, 140303 (2015).
[19] F. Giustino, S. G. Louie, and M. L. Cohen, Phys. Rev. Lett. **105**, 265501 (2010).
[20] E. Cannuccia and A. Marini, Phys. Rev. Lett. **107**, 255501 (2011).
[21] G. Antonius, S. Poncé, P. Boulanger, M. Côté, and X. Gonze, Phys. Rev. Lett. **112**, 215501 (2014).
[22] E. A. Ekimov, V. A. Sidorov, E. D. Bauer, N. N. Mel'nik, N. J. Curro, J. D. Thompson, and S. M. Stishov, Nature **428**, 542 (2004).
[23] M. Schwoerer-Böhning, A. T. Macrander, and D. A. Arms, Phys. Rev. Lett. **80**, 5572 (1998).
[24] E. Bustarret, Physica C **514**, 36 (2015).
[25] L. Boeri, J. Kortus, and O. K. Andersen, Phys. Rev. Lett. **93**, 237002 (2004).
[26] X. Blase, C. Adessi, and D. Connétable, Phys. Rev. Lett. **93**, 237004 (2004).
[27] K.-W. Lee and W. E. Pickett, Phys. Rev. Lett. **93**, 237003 (2004).
[28] Y. Ma, J. S. Tse, T. Cui, D. D. Klug, L. Zhang, Y. Xie, Y. Niu, and G. Zou, Phys. Rev. B **72**, 014306 (2005).
[29] F. Giustino, J. R. Yates, I. Souza, M. L. Cohen, and S. G. Louie, Phys. Rev. Lett. **98**, 047005 (2007).
[30] B. Sacépé, C. Chapelier, C. Marcenat, J. Kačmarčik, T. Klein, F. Omnès, and E. Bustarret, Phys. Status Solidi A **203**, 3315 (2006).
[31] P. Achatz, F. Omnès, L. Ortéga, C. Marcenat, J. Vacík, V. Hnatowicz, U. Köster, F. Jomard, and E. Bustarret, Diam. Relat. Mater. **19**, 814 (2010).
[32] See Supplemental Material at `tobeaddedbypublisher`.
[33] J. Kulda, H. Kainzmaier, D. Strauch, B. Dorner, M. Lorenzen, and M. Krisch, Phys. Rev. B **66**, 241202 (2002).
[34] Calculations were performed using density-functional theory [42, 43] within the Perdew-Burke-Ernzerhof generalized-gradient approximation [44] for the exchange-correlation functional, as implemented in `Quantum Espresso` [45]. We used a plane-wave basis set with a kinetic energy cutoff of 60 Ry, norm-conserving Goedecker-Hartwigsen-Hutter-Teter pseudopotentials [46], and a 8×8×8 Monkhorst-Pack grid for sampling the Brillouin zone. Adiabatic phonon frequencies and eigenvectors were computed through density-functional perturbation theory [47] on a 6×6×6 grid. Electron bands, phonon dispersions, and electron-phonon matrix elements were interpolated using maximally localized Wannier functions [48, 49], and Eq. (1) was computed using `EPW` v4 [50, 51]. The Brillouin-zone summation in Eq. (1) was evaluated using one million random **k**-points, and a broadening parameter $\hbar\eta = 10$ meV. In all calculations, doping with boron was modelled in the rigid-band approximation through a shift of the Fermi level below the valence band top. A temperature of 300 K was included via the Fermi-Dirac occupation factors in Eq. (1). To approximately account for finite energy and momentum resolution, the results of Eqs. (2)-(3) were broadened by $\Delta E = 1$ meV and $\Delta k = 0.08$ Å^{-1} via a Gaussian convolution.
[35] C. D. Clark, P. J. Dean, and P. V. Harris, Proc. R. Soc. London A **277**, 312 (1964).
[36] S. Zollner, M. Cardona, and S. Gopalan, Phys. Rev. B **45**, 3376 (1992).
[37] E. Bustarret, F. Pruvost, M. Bernard, C. Cytermann, and C. Uzan-Saguy, Phys. Status Solidi A **186**, 303 (2001).
[38] M. Ortolani, S. Lupi, L. Baldassarre, U. Schade, P. Calvani, Y. Takano, M. Nagao, T. Takenouchi, and H. Kawarada, Phys. Rev. Lett. **97**, 097002 (2006).
[39] W. L. McMillan, Phys. Rev. **167**, 331 (1968).
[40] P. B. Allen and R. C. Dynes, Phys. Rev. B **12**, 905 (1975).
[41] D. J. Scalapino, Y. Wada, and J. C. Swihart, Phys. Rev. Lett. **14**, 102 (1965).
[42] P. Hohenberg and W. Kohn, Phys. Rev. **136**, B864 (1964).

[43] W. Kohn and L. J. Sham, Phys. Rev. **140**, A1133 (1965).
[44] J. P. Perdew, K. Burke, and M. Ernzerhof, Phys. Rev. Lett. **77**, 3865 (1996).
[45] P. Giannozzi *et al.*, J. Phys.: Condens. Matter **21**, 395502 (2009).
[46] C. Hartwigsen, S. Goedecker, and J. Hutter, Phys. Rev. B **58**, 3641 (1998).
[47] S. Baroni, S. de Gironcoli, A. Dal Corso, and P. Giannozzi, Rev. Mod. Phys. **73**, 515 (2001).
[48] N. Marzari, A. A. Mostofi, J. R. Yates, I. Souza, and D. Vanderbilt, Rev. Mod. Phys. **84**, 1419 (2012).
[49] A. A. Mostofi, J. R. Yates, Y.-S. Lee, I. Souza, D. Vanderbilt, and N. Marzari, Comp. Phys. Commun. **178**, 685 (2008).
[50] F. Giustino, M. L. Cohen, and S. G. Louie, Phys. Rev. B **76**, 165108 (2007).
[51] S. Poncé, E. Margine, C. Verdi, and F. Giustino, Comp. Phys. Commun. **209**, 116 (2016).